ELSEVIER

Spectrochimica Acta Part B 56 (2001) 1459–1472

SPECTROCHIMICA ACTA PART B

www.elsevier.com/locate/sab

Spectroscopic investigation of the technique of plasma assisted pulsed laser deposition of titanium dioxide

A. De Giacomo[a,b,*], V.A. Shakhatov[c], G.S. Senesi[c], S. Orlando[d]

[a] *Dipartimento di Chimica, University of Bari, Via Orabona 4, Bari, Italy*
[b] *Centro di Studio per la Chimica dei Plasmi del CNR, Via Orabona 4, 70126 Bari, Italy*
[c] *Centro Laser, S.P. per Casamassima, km.3-70010 Valenzano, Bari, Italy*
[d] *CNR-IMS, Zona Industriale Tito Scalo, 85050 Tito Scalo, PZ, Italy*

Received 28 February 2001; accepted 22 June 2001

Abstract

The characterization of plasma assisted pulsed laser deposition (PA-PLD) of titanium dioxide with biased substrate is discussed. Both the stage of plasma expansion and deposition have been studied. Optical emission spectroscopy was employed to estimate laser-induced plasma parameters, while different techniques [optical microscopy, scanning electron microscopy (SEM), spectrophotometry, X-ray photoelectron spectrometry (XPS)] were used to characterize the film properties. It is shown that PA-PLD prevents contamination of the deposited films by particles ejected during the interaction of the KrF excimer laser radiation with the titanium dioxide targets. Investigation made on the film deposited by conventional PLD and PA-PLD, has shown that the PA-PLD technique allows to improve the quality of the deposited films for what concerns their stoichiometry, morphology and deposition rate.

Keywords: Plasma assisted pulsed laser deposition; Titanium dioxide; Optical emission spectroscopy; Particle elimination

* Corresponding author. Tel.: +39-080-4674-314; fax: +39-080-4674-457.
E-mail address: adg@mail.centrolaser.it (A. De Giacomo).

0584-8547/01/$ - see front matter
PII: S0584-8547(01)00274-9

1. Introduction

An important application of the interaction of high-powered laser light with condensed matter is pulsed laser deposition (PLD) [1,2]. It has becoming increasingly popular as a method for producing thin films of classical and novel materials. One of the most significant advantages of using the laser ablation technique for thin film growth is that the source of energy is external to the vacuum chamber and so it provides a much greater degree of flexibility in the selection of materials and geometrical arrangements. Moreover, almost any condensed matter material can be ablated and the amount of material deposited can be easily controlled by an appropriate adjustment of the experimental parameters such as laser fluence, background gas pressure, deposition time, etc.

The PLD process can be divided in different stages: the laser ablation of the target; the plasma generation; the plasma expansion; and the deposition of ablated species on the substrate.

The stage of the plasma generation and the plasma expansion play a very important role in the thin film growth process. In fact, during the time evolution of the laser-induced plasma (LIP), excitation and ionization of the evaporated material occurs so that the depositing material is energetically suitable for the film formation. It is important, then, to define the thermodynamic parameters of LIP such as electron number density N_e, neutral number density N, temperatures of the electrons T_e, of the atoms T_a and of the ions T_i. For the characterization of the thermodynamic parameters of LIP, optical emission spectroscopy (OES) is the most used technique [3–8]. It is based on the study of the spectral distribution of the line intensity and broadening of the emission spectra. OES allows the measurements of several important parameters of the LIP as the internal temperature of atomic and ionic species, the electron number density N_e and the expansion rate of LIP. The validity of the technique is based on some assumptions: the existence of local thermodynamic equilibrium (LTE) conditions; and the optically thin plasma. On the other hand, the detection of Stark broadening and displacement of the spectral lines allows estimating electron number density without considering LTE. The stage of excitation of the LIP consists of a set of kinetic processes that influence the populations of atoms and ions in electronically-excited states. The parameters of the LIP quickly vary owing to its expansion at low background pressure. This variation can bring to a non-equilibrium of the forward and backward kinetics processes and so, deviations from LTE conditions can occur [9]. In these conditions, electron, ion and atom temperatures can essentially differ. In this case, suitable theoretical models are needed to interpret the spectroscopic measurements [10].

In spite of mentioned advantages, PLD presents some critical drawbacks in the deposition stage, that limit the industrial interest to a few applications in the electronic field [2]. The most fundamental disadvantage in this technique is the production of macroscopic ejects during the ablation process [1,2]. This is particularly evident for target materials of high refractive index, as TiO_2, since the penetration of laser radiation into the target bulk results in the sublimation of internal layers, with the consequent macroscopic ejection of superficial material. For instance, in high performance optical applications, stringent constrains exist for the smoothness of the surface, with the result that the tolerance of particulate density and size is very low.

A number of mechanical approaches and entwined techniques has been attempted for the solution of this problem [1]. Among them, one of the simplest and the most promising techniques is the plasma assisted pulsed laser depositon (PA-PLD), where an additional plasma discharge is created between the target and the substrate in the presence of a background gas [1,11]. Sankur and Gunning [12] have found that the use of PA-PLD improves the optical properties of a titanium dioxide film. This cross-bred technique based on PLD have been pursued to either enhance the process capabilities or to modify the properties of materials such as superconducting [13–15], diamond-like carbon [16] and titanium

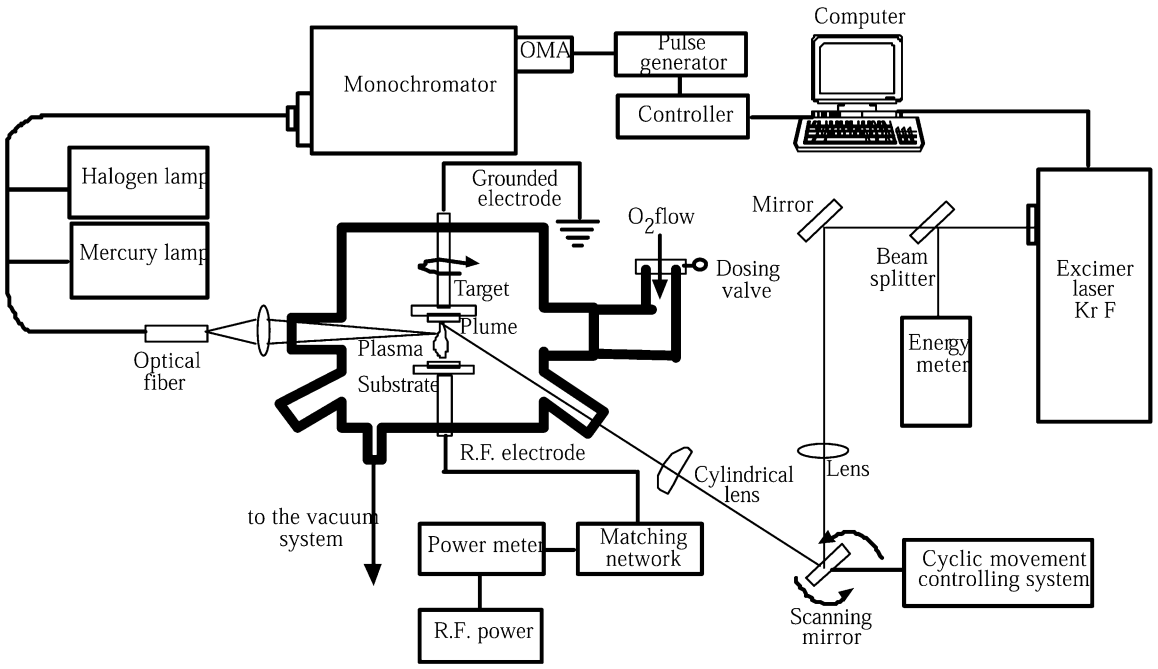

Fig. 1. Experimental set-up.

dioxide (TiO_2) [17]. In most of these experiments, film deposition was performed by PLD in the presence of a plasma discharge, which was initiated inside the chamber and was sustained under an appropriate bias voltage applied to the electrode placed between the target and the substrate. Films deposited with this technique were characterized by an improvement in either their uniformity and homogeneity or in their morphology and crystallinity. The analysis of the experimental material obtained demonstrates that the plasma effects on the film properties are dependent on the plasma discharge excitation method.

In this paper we present the results of measurements made by time and spatially resolved emission spectroscopy of the time evolution of the electron number density and of atomic and ionic state distribution functions (ASDF and ISDF) in the LIP occurring as results of the interaction of a KrF excimer laser irradiation with TiO_2 targets at the different values of laser fluence (from 0.8 to 6 J/cm^2), of the oxygen pressure (from 10^{-6} to 10^{-1} torr) and distances from the targets (from 0.6 to 6 mm). Moreover, the aim of this work is to show that PA-PLD, in parallel plates configuration, allows to decrease markedly particle formations in thin films for optical applications and to improve the quality of the deposited film for what concerns its stoichiometry, morphology and deposition rate.

2. Experimental set-up

The experimental set-up consists of an excimer laser with an optical system in order to steer and focus the laser beam, a PLD vacuum chamber, a system for gas feeding and pumping out and a pressure controlling system and a spectroscopic system, as depicted in Fig. 1.

A pulsed KrF excimer laser, with an emission wavelength of 248 nm, is used as the source of monochromatic radiation for evaporating the target material. The laser is operated at a repetition rate of 10 Hz, with a pulse duration of 30 ns. The

energy of the laser is varied up to 1.5 J and is controlled by means of an energy meter. Using mirrors and spherical lenses, the laser beam is directed through a quartz window into the PLD chamber and focused onto a target at 45° from the surface normal to reduce the plasma shield effect on the incoming laser pulse. The fluence of the laser beam is varied up to 6 J cm^{-2}, by adjusting its degree of focusing on the target and the laser energy output.

The PLD chamber is a typical stainless steel vacuum chamber of cylindrical geometry. It is equipped with holders for the target and the substrate, ports for the laser beam, gas pumping out and feeding and pressure gauging. The distance between the target and substrate is fixed at 3 cm. The thin films are grown under non-excited oxygen flow or under oxygen r.f. discharge. The r.f. discharge is created into the PLD chamber by means of a r.f. power supply (27 MHz, 100 W). The r.f. discharge geometry is a simple parallel plates design, where the substrate is connected to the r.f. electrode and target to the grounded electrode. In this way, a visible discharge surrounds the plume expansion. The typical self-bias induced by the r.f. power generator, allows an acceleration of the ionic species directed to the substrate surface, causing its activation. The target holder is continuously rotated to avoid the formation of laser-induced craters locally on the target.

In order to obtain an homogeneous flux of the background gas during the experiments, an aperture of 3 cm of a quartz tube connected to the feeding valve is used. The chamber is pumped down to 10^{-6} torr by rotary and turbo-molecular pumps.

The emission spectrum from the LIP is detected by two different methods. Time-integrated optical emission spectroscopy is utilized to identify chemical species generating in the laser-induced plume and to investigate LIP until 6 mm from the target. Spatially-and-temporally resolved optical emission spectroscopy is used to investigate the time evolution of the spectral line intensity and broadening, ASDF and ISDF, and to estimate electron number density depending on time, close to the target (0.6 mm).

To record a spectral distribution of the line intensity in emission spectra, in a range of wavelengths from 250 to 700 nm, a high resolution monochromator is applied (HR 640, Instruments S.A., division Jobin Yvon) equipped with a holographic grating 2400 g/mm and an intensified charge coupled device (ICCD, ORIEL Instruments), for time resolved measurements or an optical multichannels analyzer (OMA IRY 700 GmbH), for time integrated measurements.

The detection of the ICCD output signal is accomplished by a Stanford Research DG 535 programmable pulse generator, connected through a general purpose interface bus (GPIB), to a personal computer (PC) for data acquisition and processing. To exclude a timing jitter of the excimer laser and spectroscopic systems, a portion of the laser beam by glass wedge is split off and detected by a fast photodiode in order to trigger the pulsed generator. A digitizing fast oscilloscope (Tektronix TDS 620 A) and a photodiode are used to calibrate and control the gate width and time delay after the laser irradiation.

A gate width of 15 ns is used to maximize the spectral line intensity while maintaining good temporal resolution. Accuracy in establishment of a time delay t_d is 4 ns for a range from 100 to 600 ns. To optimize the signal-to-noise ratio, the detection of signals is carried out in accumulation mode. The average value of the signal from the laser-induced plasma is obtained over 20 consecutive laser pulses in time integrated OES and 150 consecutive laser pulses in time resolved OES, at the repetition rate of 10 Hz.

A quartz lens optically projects the plume image of the LIP, with 1:1 magnification, on the entrance of an optical fiber placed outside of the deposition chamber. So the UV-grade optical fiber (core diameter 0.6 mm) is placed on the image plane of the plume and it is mounted on an optical table, permitting vertical and horizontal micro-movements to collect light emitted from different regions of the LIP. The aperture of the optical fiber is aligned with centerline of the plume to ensure that the emission signal is collected perpendicular with respect to its symmetry axes.

The output of the optical fiber is coupled to the slit of the monochromator. The slit width is set at 100 μm. The maximum spectral resolution of the optical system is determined as 0.2 Å monitoring the lines of a mercury lamp and an He–Ne laser for the slit width used in the experiment. The spectral response of the optical system including lens, optical fiber, monochromator and detector is controlled with a tungsten halogen lump. To investigate the spectral contour and width of the investigated lines the instrumental function of the optical system was measured by the mercury lamp and a He–Ne laser. The line profile is well fitted by a Voight profile, characterized by a spectral width 0.9 ± 0.08 Å (FWHM). ASDF and ISDF are recovered from relative atomic and ionic line intensity measurements [16,17]. For each selected spectral line, a computer code calculates the area by the fitting of spectral line contours with an automatic baseline correction.

A scanning electron microscope (SEM) is used to analyze highly polished thin sections of the deposited film surfaces. The stoichiometry of films were controlled by X-ray photoelectron spectroscopy (XPS) measurements. Optical transmittance of TiO_2 films was analyzed by a spectrophotometer.

The thickness of obtained films was measured with a profilometer and so the deposition rate was obtained by the ratio between the thickness of films and the deposition time.

3. Results and discussion

3.1. Optical emission spectroscopy of titanium dioxide LIP

The emission spectra of LIP has been observed at different distances from the target and delay time from the laser pulse, in order to characterize the thermodynamic and the kinetic of the processes involved as a result of the interaction of laser radiation with TiO_2 target. A series of characteristic titanium lines was observed and interpreted as emission from the excited neutral atoms and from single charged ions (Ti-I and -II). Spectral lines corresponding to the transitions between the excited states of the oxygen atoms O I and ions O II, were not observed because their intensities are too low with respect to the corresponding ones of the Ti-I and -II lines, or that they are overlapped by too-strong close to each other lines, to be clearly identified in the spectral range investigated (250–700 nm). In addition, no molecular

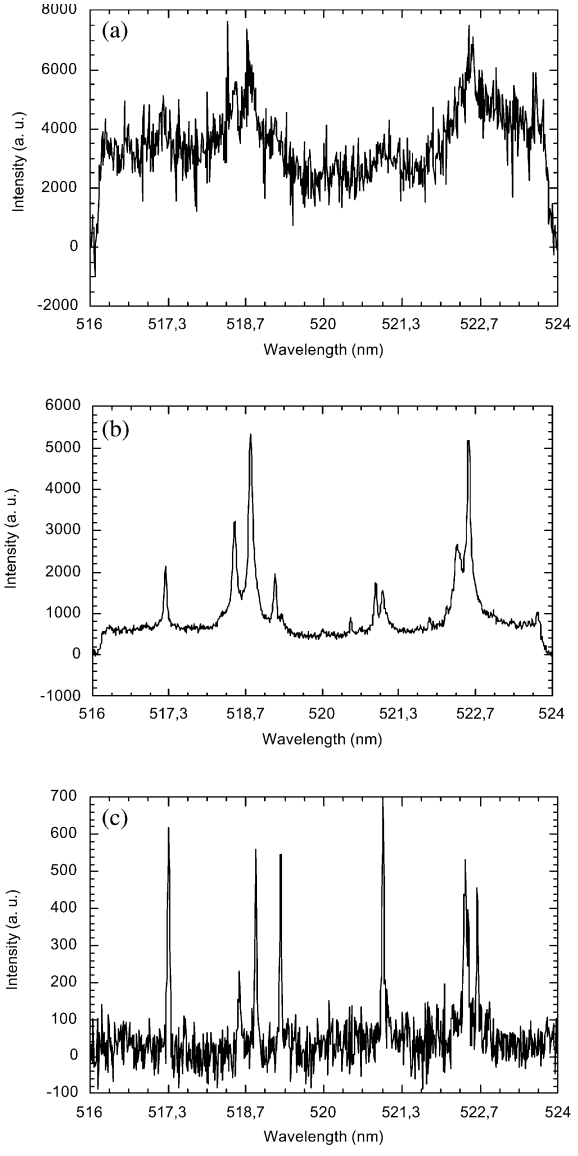

Fig. 2. Fragment of time integrated spectra of LIP in vacuum at different distance: (a) $d = 0$ mm; (b) $d = 2$ mm; and (c) $d = 6$ mm.

species such as TiO, TiO_2, O_2 or molecular oxygen ions were observed in the LIP at the distances from the target investigated in the present work (until 6 mm) in accordance with [6,18]. After the identification of the spectral lines, in order to determine titanium ASDF and ISDF evolution during LIP expansion, several lines not overlapping with nearby lines and having emission times shorter or at least comparable with the time of residence of the LIP in the probe volume, were chosen.

Fig. 2 shows the time integrated spectra of LIP as function of distance, while Fig. 3 shows the temporal evolution of a typical fragment of LIP spectrum collected by a temporal resolution of 15 ns. As can be observed the spectra (within a spatial resolution of 0.5 mm) declines rapidly as a consequence of the LIP expansion. Note that in the case of time resolved spectra, the detection began after 100 ns from the laser pulse at 0.6 mm from the target, because spectral lines arise clearly only at this time from the initial continuum spectra due to collisions of free electrons with heavy particles and radiative recombination of electrons with positive ions.

The velocity of LIP expansion was estimated by time of flight (TOF) [1,15,19] measurements, monitoring emission of selected atomic lines and is reported at different distances in Fig. 4. As will be explained below for atomic species a correction for spontaneous emission is needed. The curves show the temporal distribution of titanium atoms, for crossing the aperture of the optical fiber (0.06 cm) placed in the 1:1 virtual plane. Up

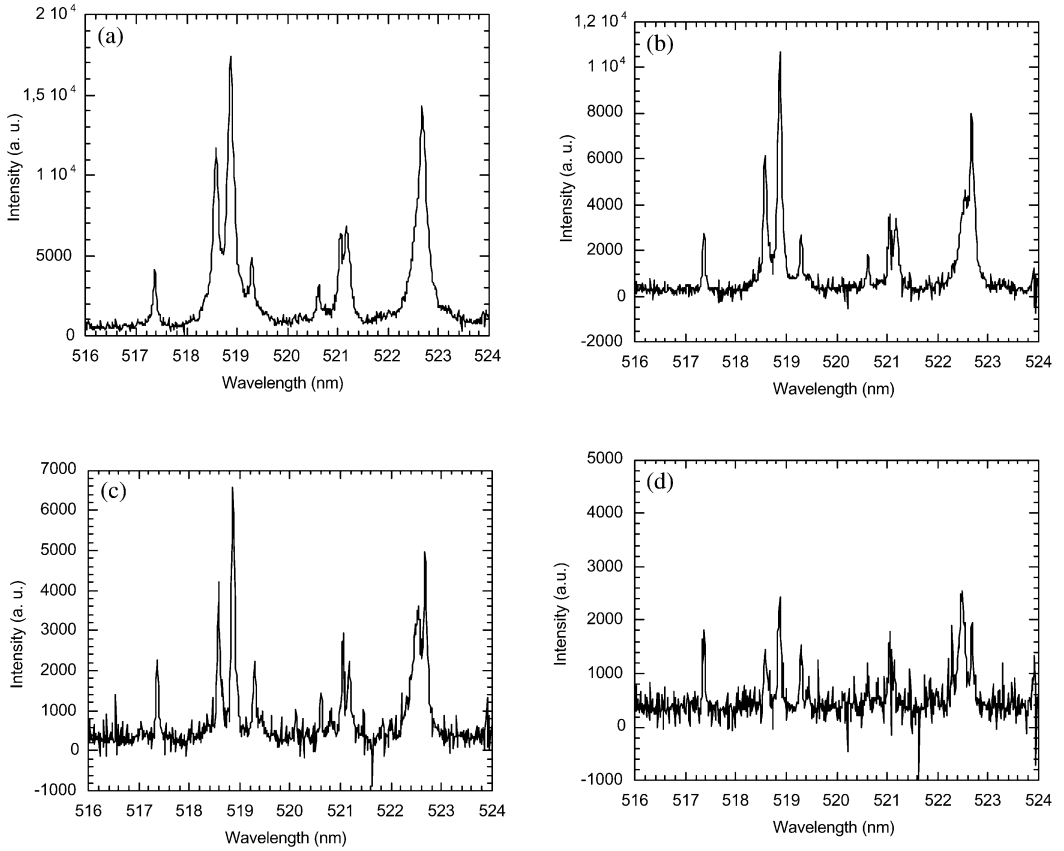

Fig. 3. Fragment of time resolved spectra of LIP, in vacuum at 0.6 mm from the target, at different delay time: (a) $t = 100$ ns; (b) $t = 160$ ns; (c) $t = 220$ ns; and (d) $t = 300$ ns.

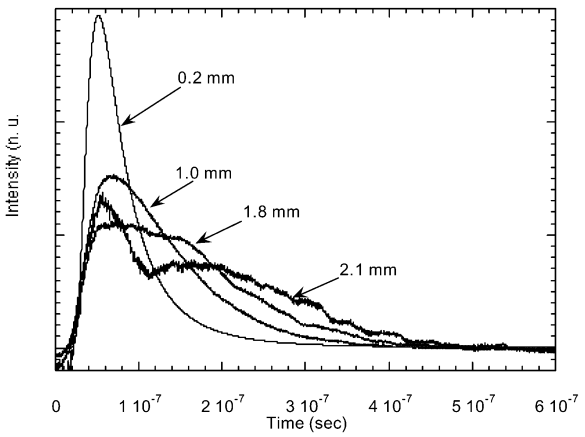

Fig. 4. TOF measurements of Ti-I lines at different distances, at the laser fluence of 3 J cm^{-2}.

to 1 mm from the target, the temporal distribution is Maxwellian and the velocity of expansion so measured is 1.3×10^6 cm/s at 0.2 mm from the target. This result was confirmed by the empirical method reported in [4], here the authors estimated the rate of expansion by the difference in time between the maxima of two TOF curves obtained at a known different position. In this way the ratio between the difference in distance and the difference in time gives a mean velocity that is not affected by instrumental questions.

Observing Fig. 4, it is evident that the distribution of velocity becomes progressively broader with the distance from the target, because of collisions and diffusion of heavy particles during the LIP expansion. Increasing the background oxygen pressure, the broadening of TOF signal happens for shorter distances [15,19]. This is reflected on the shape of plume that changes from a cone geometry in vacuum to a pear shape in background gas.

The electron number density was determined experimentally by the quadratic stark broadening [20,21] considering a Voigt shape of the spectral lines and it varies between 10^{18} and 10^{16} cm^{-3} during the temporal evolution of LIP from 100 to 300 ns, at the laser fluence of 6 J cm^{-2}. An example of the temporal dependence of spectral line shape is presented in Fig. 5, where the line width decreases rapidly as a function of time, from their maximum value of 1.5 A at 100 ns to 0.9 A at 280 ns, which coincide with the width of the instrument function of our spectroscopic equipment.

The whole luminosity of the plume, close to the target, increases with oxygen pressure, because of the collision of the expanding LIP with the oxygen background gas. Therefore, 2 mm far from the target, the spectral line intensity slightly decreases (Fig. 6) in accordance with [22], while the line shape is not influenced by the oxygen pressure close to the target.

To estimate the thermal energy and to charac-

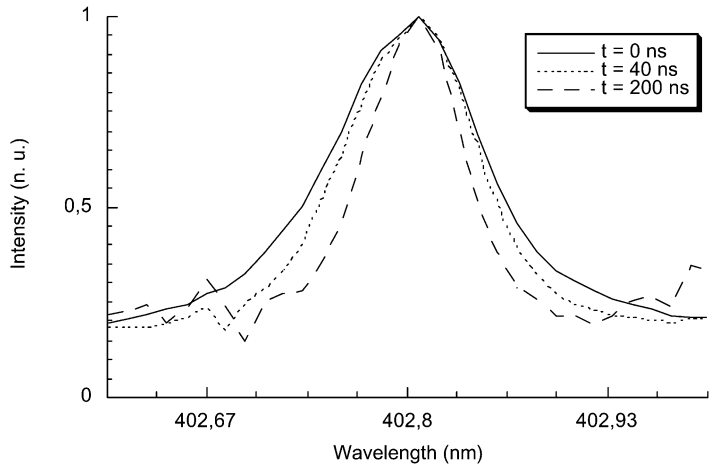

Fig. 5. Line shape of Ti-I 402.7 at a different delay time detected with the gate width of 15 ns.

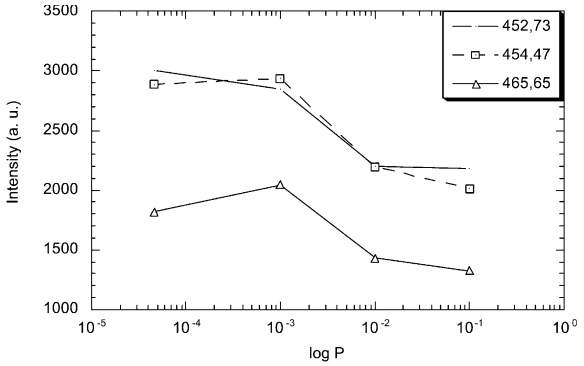

Fig. 6. Time integrated spectral line intensity, at 452.7, 454.5 and 465.65 nm, as a function of pressure at the target distance of 2 mm.

terize the thermodynamic conditions of the LIP, the distribution functions of the electronic excited states of titanium atoms and ions were recovered from the experimental spectra at different values of laser fluence and oxygen pressure under non-excited oxygen flow and under r.f. oxygen discharge. Fig. 7a,b shows, as an example, the time integrated measured distribution functions, at 2 mm from the target of Ti-I and -II, which can be represented, in good approximation, in a Boltzmann form. So, assuming a Boltzmann distribution, the temperatures of Ti-I and -II, corresponding to each measured distribution function, can be determined using the Boltzmann plot technique [23] by the measurements of intensities of the spectral lines I_{nm} by the following equation:

$$\ln\left(\frac{I_{nm}}{g_m \cdot \nu_{nm} \cdot A_{nm}}\right) = -\frac{E_m}{k \cdot T_i} + \ln\left(\frac{N_i}{Z_i}\right)$$

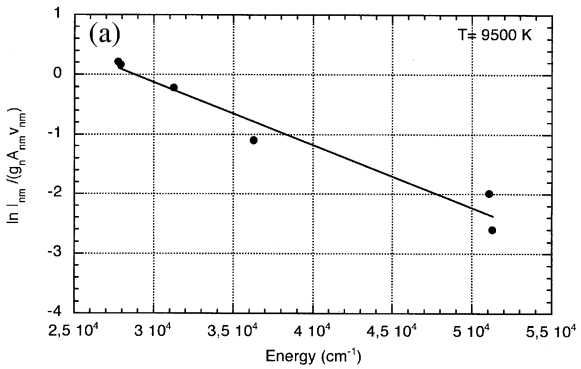

Fig. 7. Time integrated Boltzmann plot at 2 mm from the target of (a) Ti-I and (b) Ti-II.

where k is the Boltzmann's constant, ν_{nm} is the frequency of the photons emitted by the transition from the upper excited energy level E_m to the lower energy level E_m, Z_i is the partition function of the chemical species i calculated at T_i, N_i is the concentration of the chemical species i in the ground state. This equation can be used to build up a plot of $\ln(I_{nm}/g_m\ \nu_{nm}\ A_{nm})$ vs. the

Table 1
Temporal evolution of Ti-I and Ti-II excitation temperature[a]

Delay time t_D	T_I (K)	T_i^* (K)	T_a (K)	T_a^* (K)
100	30 850	29 122		
140	27 230	26 795	12 850	14 918
180	22 730	24 102	11 260	13 204
220	19 300	21 163	9735	11 490
260	16 180	18 102	10 310	11 122
300	14 370	14 061	10 890	11 100

[a](t_D) is the delay time from the laser pulse, T_i and T_a are the experimental value with a relative error of 15% and T_i^* and T_a^* are the calculated values by the model reported in [10], respectively, for ions and for neutral.

Table 2
Ti-I and -II excitation temperature at different distance[a]

d (mm)	T_a (K)	T_i (K)
0	10 948	14 200
2	9479	13 503
6	8822	12 886

[a] d is the distance from the target T_a and T_i are the experimental value with a relative error of 15%, respectively, for neutral and for ions.

energy E_m appropriate to the experimental points by means of the least-square fitting method. For this proposal it used spectral data reported by [24]. The plot gives a straight line whose slope is proportional to the inverse of excitation temperature. The time resolved measurements of the excitation temperature, showed in Table 1, put in evidence that, at 0.6 mm from the target, after 100 ns from the laser pulse, a significant difference between the temperatures of Ti-I and -II arises as consequence of the expansion of the LIP at low pressure. As will be explained below, also if the electron number density is high ($> 10^{15}$ cm^{-3}) and the Boltzmann distribution is assumable for titanium species, the LTE assumption is not valid, because the expansion rate is so fast that different kinetic processes roles take place for atoms and ions. The same phenomena are observed by spatial resolved measurement performed by integrated time OES and reported in Table 2.

In order to explain the discrepancy in atomic and ionic excitation temperature, a collisional radiative model described in detail in a previous work [10], was applied to the experimental results in vacuum. In this model were considered the collisional excitation and de-excitation of atoms and ions with electrons, collisional ionization and three bodies' recombination, radiative recombination and photo-ionization, spontaneous emission, reabsorption and stimulated emission. After 100 ns from the laser pulse, the calculation showed that ASDF and ISDF are governed mainly by the process of excitation and de-excitation of atoms and ions with electrons and by the radiative processes, such as spontaneous emission, reabsorption and stimulated emission. All the other processes are negligible at this stage of the LIP expansion. In particular, the ASDF time evolution is mainly governed by excitation and de-excitation of the electronically excited states by electron impact and decay by spontaneous emission, while for ISDF, along with the above mentioned processes, process of reabsorption play an important role. The fitting of experimental measurements by the results of the theoretical model demonstrates that the different roles of the radiative processes for ions and atoms are the cause of the discrepancy in the excitation temperature of ions and atoms. Using the results of this model, a suitable correction can be applied to the ASDF

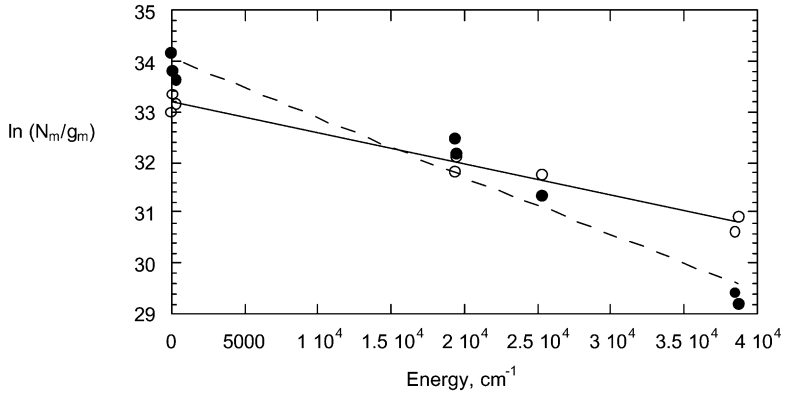

Fig. 8. Boltzmann plot, obtained by numerical simulation, of ASDF (○) and Boltzmann plot obtained after the correction for the spontaneous emission mechanism of ASDF (●).

and ISDF recovered experimentally, considering only the calculated results of ASDF and ISDF due to the channels of excitation and de-excitation by electron impact so that virtual conditions of LTE can be established. In this way, the concentration of titanium species can be estimated by the intercept of the new Boltzmann plot obtained with the ASDF and ISDF, calculated by the model taking in account only the channels of excitation and de-excitation by electron impact (Fig. 8). The concentration of titanium species and of electrons number density determined experimentally by measurements of Stark effect is showed in Fig. 9. Assuming a congruent evaporation of species from the target, a complete atomization of the material ablated and neglecting higher ionization stage, is possible to compute the concentration of oxygen species in vacuum, that are twice the concentration of titanium species. So adding the concentration of titanium and oxygen species and electron number densities recovered experimentally by the quadratic Stark effect, the pressure temporal evolution of LIP is estimated and presented in Fig. 10.

The spectroscopic investigation of the laser-induced plume emission shows that no notable thermodynamic differences are caused by the presence of the r.f. discharge during the plume

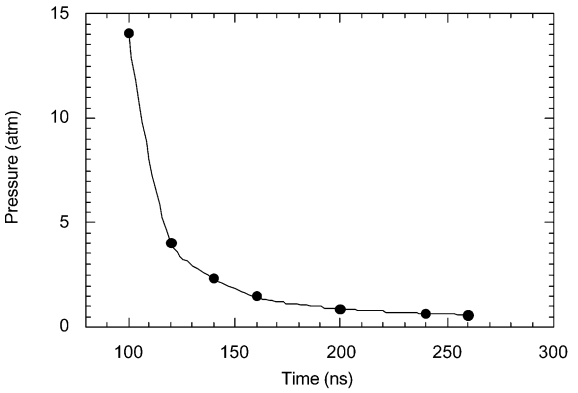

Fig. 10. Estimation of LIP pressure as a function of time.

expansion. Fig. 11 shows the temperature of excited state of titanium atoms obtained by the Boltzmann's plot technique for PLD and PA-PLD. The measure of line intensity was performed by time integrated OES in order to observe some differences in the whole expansion process. As it is observable by Fig. 11, the excitation temperatures of titanium atoms are coincident, in the range of experimental error, for both PA-PLD and PLD for a distance from the target up to 6 mm. We suggest that this result is the consequence of the large difference between the r.f. plasma and the laser-induced dense plasma parameters, as electron density, electron temperature etc. [23–27].

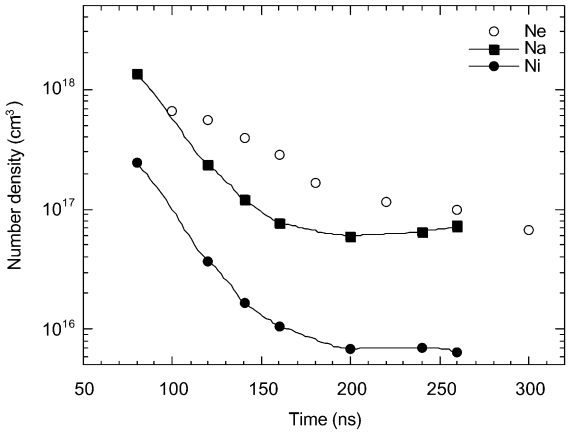

Fig. 9. Temporal evolution of Ti-I (■) and Ti-II (●) concentration, estimated by the intercept of the Boltzmann plot corrected for radiative process, and experimental electron number density (○).

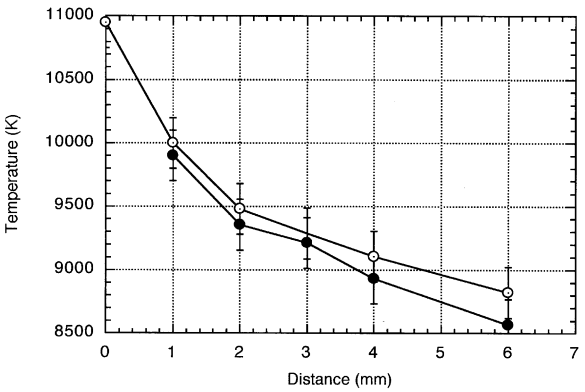

Fig. 11. Comparison of the internal temperature of titanium atom excited states as a function of distance from the target during PLD (●) and PA-PLD (○). Laser fluence = 1.3 J cm^{-2}, and oxygen pressure = 10^{-2} torr.

3.2. Characterization of titanium dioxide films deposited

The effect of the r.f. discharge on the PLD process is investigated in a range of fluence (0.8–2.5 J cm^{-2}) and oxygen pressure (7×10^{-4}–10^{-1} torr) for the production of TiO_2 film. As was mentioned above, the task of our experiment is the partial elimination of particles in view of achieving a final product suitable for optical applications. A series of films deposited at different pressure and laser fluence conditions is investigated by SEM and the particles observed are catalogued in three different typologies based on their size (I, < 20 μm, II, 0.8–2 μm, III, < 0.2 μm).

It is possible that the first and the second type of particles are ejected by spalling of target material [1], whereas the third type of particles are originated by hydrodynamic sputtering of target as well as by the liquid ejection. At highest fluence (> 2 J cm^{-2}), the nature of particles change in larger particles (15–20 μm), suggesting the splashing of melt drops.

Fig. 12a,b shows images captured by an optical microscope. The reduction of particles occurred on the surface and in the bulk of PA-PLD film is observed.

We suppose that atomic species and mainly molecular ions of the r.f. discharge are accelerated by the plasma self-bias to the r.f. powered electrode and to the substrate, thus activating its surface and destroying large particles. So, on the other hand, it is possible that large particles, negatively charged for the fast electron diffusion effect, are rejected by the r.f. electrode and therefore, deviated to the border of the substrate. Indeed, a few micro-particles are also observable in films obtained by PA-PLD.

The presence of an active oxygen environment excited by the r.f. discharge [12] during the production of oxide films presents, as another advantage, the possibility of working at a lower background oxygen pressure without losing the stoichiometric oxygen content in the film deposited. The possibility of using a lower pressure of the background gas enhance the deposition rate, as it is observable in Fig. 13, which shows the deposition rate for PLD and PA-PLD. Without the r.f. discharge, it is necessary to increase the background oxygen pressure up to 10^{-2} torr to achieve a stoichiometric TiO_2 film. As demonstrated by XPS analysis [11], the same stoichiometry is available for PA-PLD at 7×10^{-4} torr because the oxygen is activated and ionized by the r.f. discharge. Moreover, oxygen ions are incorporated in the film as consequence of self-bias effect. The deposition rate for conventional PLD at 7×10^{-4} torr is extremely low because small amounts of

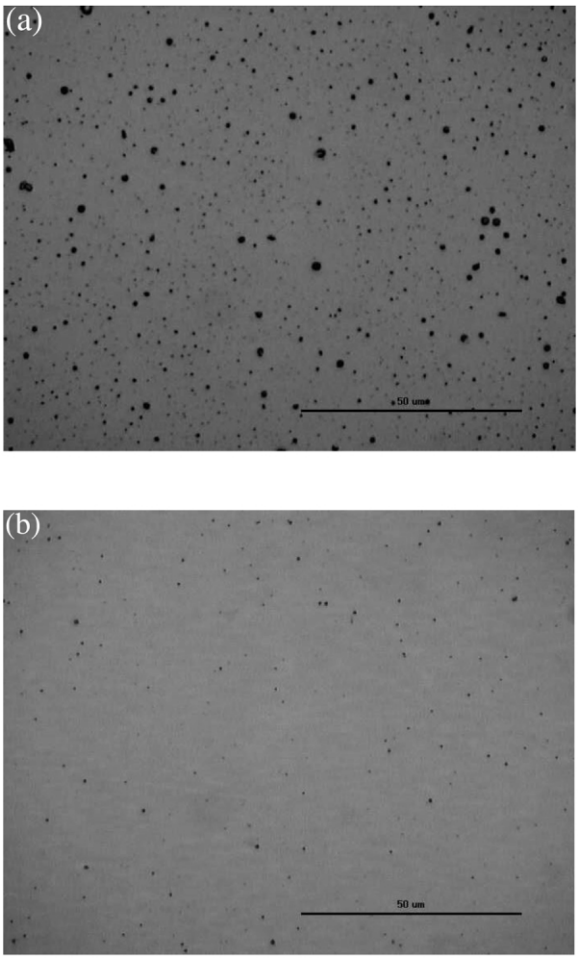

Fig. 12. (a) Optical microscopy image of film obtained by conventional TiO_2 PLD process at the laser fluence of 1.3 J cm^{-2} and oxygen pressure of 10^{-2} torr. (b) Optical microscopy image of film obtained by TiO_2 PA-PLD process at the laser fluence of 1.3 J cm^{-2} and oxygen pressure of 10^{-2} torr.

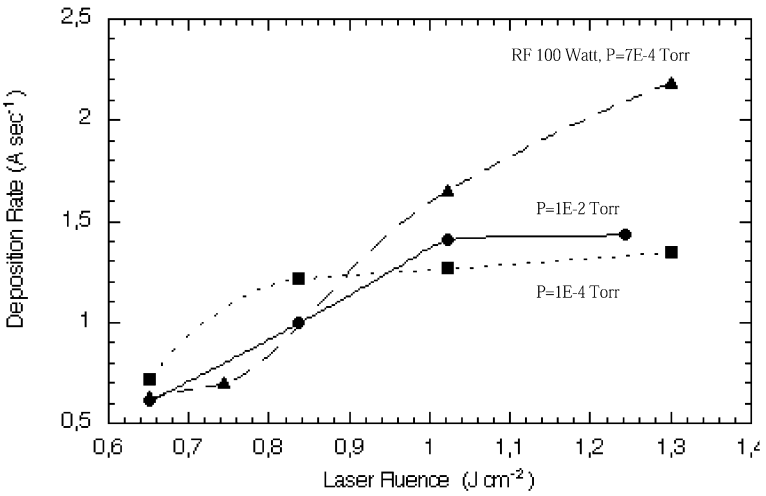

Fig. 13. Deposition rate of films deposited by PA-PLD at 7×10^{-4} torr (▲), by PLD at 10^{-2} torr (●) and at 7×10^{-4} torr (■).

oxygen are incorporated in the deposited film, making it unsuitable for optical application.

The morphologic and stoichiometric improvements are reflected in the optical property estimated by transmittance measurement and shown in Fig. 14a,b, where transmission ratio of films deposited by PA-PLD and PLD is reported. The improvement of transmittance proves the film obtained by PA-PLD is better for what concerns both the stoichiometry and the reduction of particulate.

Since the spectroscopic investigation of the LIP shows that no notable thermodynamic difference are caused by the presence of the r.f. discharge, but great difference are observed in the property of film deposited, we suppose that the main effect of the r.f. discharge should occur during the deposition stage where activated oxygen species interact with the front head of the LIP and with the substrate surface.

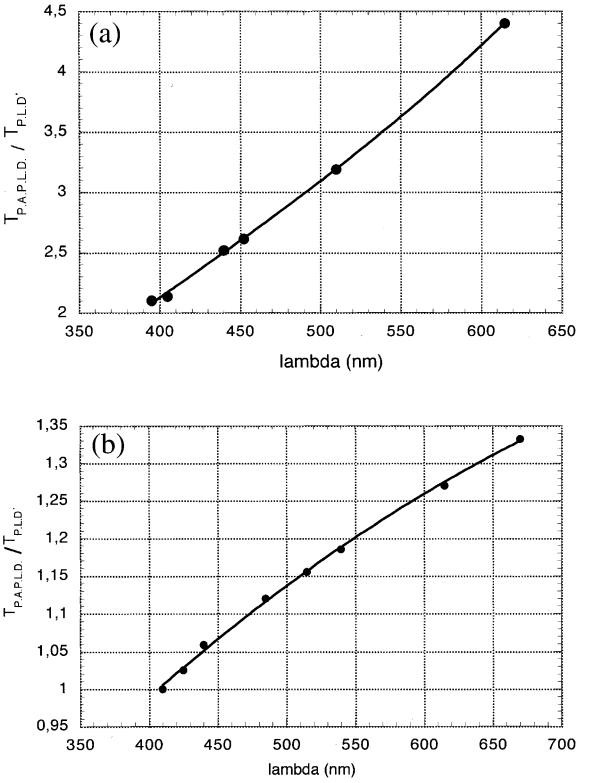

Fig. 14. (a) Optical transmission ratio of TiO_2 films obtained by PA-PLD and PLD as a function of wavelength. (Deposition condition: laser fluence 1.3 J cm^{-2}; and oxygen pressure 7×10^{-4} torr.) (b) Optical transmission ratio of TiO_2 films obtained by PA-PLD and PLD as function of wavelength. (Deposition condition: laser fluence 1.3 J cm^{-2}; and oxygen pressure 10^{-2} torr.)

4. Conclusion

The LIP thermodynamic and kinetic characteristics in PLD and PA-PLD have been studied. Electron, neutral and ionic number density and internal temperature of titanium species was esti-

mated by OES at different experimental conditions. No notable differences have been found in spectroscopic observation of LIP when PLD and PA-PLD were employed. These results were explained by the different characteristics of plasmas obtained by laser and by r.f. discharge. In spite of this, it has been observed that the r.f. discharge affects the PLD process improving the film morphology by a partial elimination of particles. It was shown that particles over micron size are totally removed and other particles are notably reduced. It was established that PA-PLD improves the quality of the TiO_2 deposited film for what concerns the stoichiometry, the morphology and the deposition rate. Finally, we suppose that the r.f. discharge effect plays an important role in the deposition stage because atomic species and mainly molecular ions of the r.f. discharge are accelerated by the plasma self-bias to the r.f. powered electrode and to the substrate, thus activating its surface and destroying large particles. The PA-PLD technique has been applied to other substrates, as Praseodymium doped chalcogenide glass, and the same improvement in film deposited has been observed.

Acknowledgements

This work was supported by CNR/P.F. Materiali Speciali per Tecnologie Avanzate (contract N° 97.01005.34). The authors are grateful to Prof. M. Capitelli, Dr G. Colonna and Dr A. Casavola for showing interest in this study and for taking part in our discussion.

References

[1] D.B. Chrisey, G.K. Huber, Pulsed Laser Deposition of Thin Films, A Wiley-Interscience Publication, 1987.

[2] P.R. Willmott, J.R. Huber, Pulsed laser vaporization and deposition, Rev. Modern Phys. 72 (1) (2000) 315–328.

[3] S.S. Chu, M. Ye and C.P. Grigoropoulos, Spectroscopic characterization of laser-induced titanium plume, Proccedings of the 5th ASME/JSME, San Diego, California, USA, March 15–19, 1999, pp. 1–5.

[4] X.T. Wang, B.Y. Man, G.T. Wang, Z. Zhao, B.Z. Xu, Y.Y. Xia, L.M. Mei, X.Y. Hu, Optical spectroscopy of plasma produced by laser ablation of Ti alloy in air, J. Appl. Phys. 80 (3) (1996) 1783–1786.

[5] B.Y. Man, Particle velocity, electron temperature, and density profiles of pulsed laser-induced plasmas in air at different ambient pressures, Appl. Phys. B 67 (1998) 241–245.

[6] M.H. Hong, Y.F. Lu, T.M. Ho, L.W. Lu and T.S. Low, Plasma diagnostics in KrF excimer laser deposition of Ti thin films, in: D. Shu-Sun and S.L. Wang (Eds.), Laser Processing of Materials and Industrial Application II: Proccedings of SPIE 3550, 1998, p. 441.

[7] F. Fuso, L.N. Vyacheslavov, G. Masciarelli, E. Arimondo, Stark broadening diagnostics of the electron density in the laser ablation plume of $Yba_2Cu_3O_{7-x}$ and $PbZr_xTi_{x-1}O_3$, J. Appl. Phys. 76 (12) (1994) 8088–8096.

[8] O.A. Bukin, I.V. Bazarov, N.S. Bodin, A.A. Il'in, V.D. Kiselev, E.A. Sviridenkov, V.I. Tsarev, A.Yu Major, Influence of the pressure of a gaseous, atmosphere on the characteristics of the emission spectra of a laser plasma generated on the surfaces of solid targets, Quantum Electron. 28 (8) (1998) 685–688.

[9] M. Capitelli, F. Capitelli, A. Eletskii, Non-equilibrium and equilibrium problems in laser-induced plasmas, Spectrochim. Acta Part B 55 (2000) 559–574.

[10] A. De Giacomo, V.A. Shakhatov, O. De Pascale, Optical emission spectroscopy and modeling of plasma produced by laser ablation of titanium oxides, Spectrochim. Acta Part B 56 (2001) 753–776.

[11] V.A. Shakhatov, A. De Giacomo, V. D'Onghia, Plasma assisted pulsed laser deposition of titanium dioxide, in: V.I. Pustolov, V. Komunov (Eds.), ALT 99 International conference: Advanced Laser Technologies: Proceedings of SPIE 4070 1999, p. 394.

[12] H.O. Sankur, W. Gunning, Deposition of optical thin films by pulsed laser assisted evaporation, Appl. Opt. 28 (14) (1989) 2806–2808.

[13] S. Witanachchi, H.S. Kwok, X.W. Wang, D.T. Shaw, Deposition of superconducting Y–Ba–Cu–O films at 400°C without post-annealing, Appl. Phys. Lett. 53 (3) (1988) 234–236.

[14] R.K. Singh, J. Narayan, A.K. Singh, J. Krishnaswamy, In situ processing of epitaxial Y–Ba–Cu–O high T_c superconducting films on (100) $SrTiO_2$ and (100) YS–ZrO_2 substrates at 400–650°C, Appl. Phys. Lett. 54 (22) (1989) 2271–2273.

[15] H.S. Kwok, H.S. Kim, S. Witanachchi, E. Petrou, J.P. Zheng, S. Patel, E. Narumi, D.T. Shaw, Plasma-assisted laser deposition of $YBa_2Cu_3O_{7-\Omega}$ Appl. Phys. Lett. 59 (27) (1991) 3643–3645.

[16] J. Krishnaswamy, A. Rengan, J. Narayan, K. Vedam, C.J. McHargue, Thin-film deposition by a new laser ablation and plasma hybrid technique, Appl. Phys. Lett. 54 (247) (1989) 2455–2457.

[17] V.A. Shakhatov, A. De Giacomo, V. D'Onghia, Plasma assisted pulsed laser deposition of titanium dioxide, In: Abstracts of the 7th International Symposium on Trends and Applications of Thin Films, Nancy, France, 28–30 March, N 295, 2000, pp. 393–395.

[18] J. Hermann, C. Dutouquet, Analyses of gas-phase reactions during reactive laser ablation using emission spectroscopy, Appl. Phys. 32 (1999) 2707–2713.
[19] J.C.S. Kools, T.S. Baller, S.T. De Zwart, J. Dieleman, Gas flow dynamics in laser ablation deposition, J. Appl. Phys. 71 (9) (1992).
[20] H.R. Griem, Spectral Line Broadening by Plasmas, Accademic Press, New York, 1974.
[21] J. Hermann, A.L. Thomann, C. Boulmer-Leborgne, B. Dubreuil, M.L. De Giorgi, A. Perrone, A. Luches, I.N. Mihailescu, Plasma diagnostics in pulsed laser TiN layer deposition, J. Appl. Phys. 77 (7) (1995).
[22] H.F. Cheng, In situ spectroscopic examination of plasma emission during excimer laser deposition of $Pb_{0.58}La_{0.05}(Zr_{0.7}Ti_{0.3})_{0.9875}O_3$ thin films, Jpn. J. Appl. Phys. 34 (10) (1995) 5751–5757.
[23] H.R. Griem, Principles of Plasma Spectroscopy, Cambridge University Press, Cambridge, 1997.
[24] C.E. Moor, Atomic Energy Levels, Volume I–III, US Department of Commerce, National Bureau of Standards, Circular, 1949.
[25] Yu.P. Raizer, Gas Discharge Physics, Springer-Verlag, 1991.
[26] R.H. Huddlestone, S.L. Leonard, Plasma Diagnostic Techniques, Academic Press, New York, London, 1965.
[27] G. Colonna, A. Casavola, M. Capitelli, Modelling of LIBS plasma expansion, Spectrochim. Acta Part B 56 (2001) 567–586.